TOWARD OBJECTIVE, STANDARDIZED INTENSITY ESTIMATES FROM SURFACE WIND SPEED OBSERVATIONS

BY FORREST J. MASTERS, PETER J. VICKERY, PHUONG BACON, AND EDWARD N. RAPPAPORT

Direct use of surface wind speed observations can introduce significant errors in storm intensity estimates without correction for terrain and instrument response characteristics.

The Automated Surface Observing System (ASOS) and its predecessor, the Automated Weather Observing System (AWOS), record surface meteorological conditions and provide minute-to-minute weather updates. Wind speed measurements collected at these sites are the focus of this study in the context of surface wind field standardization. Powell et al. (1996) demonstrated that using non-standardized data can introduce surface-layer wind speed errors on the order of 30%–40% due to terrain effects. After considering averaging techniques and anemometer response characteristics, similar errors are observed for gusts in this paper.

Using 1-min records archived in the land-based data repository at the National Climatic Data Center (www.ncdc.noaa.gov), an objective, automated, and data-driven technique is applied to estimate directional effective roughness length (z_0) values from averages of neutrally stratified mean gust factors (GFs), which are peak gust ($\hat{u}$) to mean wind speed ($\bar{U}$) ratios of stationary wind velocity segments:

$$GF(T,t,z,z_0) = \frac{\breve{u}(t,z,z_0)}{\bar{U}(T,z,z_0)}. \quad (1)$$

The GF is dependent on the instrument height z, z_0, the gust duration t, and the averaging duration T. It has been widely studied in winter storms (e.g., Durst 1960; Ashcroft 1994), thunderstorms (e.g., Choi and Hidayat 2002; Orwig and Schroeder 2007), and tropical cyclones (e.g., Krayer and Marshall 1992; Vickery and Skerlj 2005; Masters et al. 2010), and is recognized to increase with the height and density of the upwind terrain elements. A small value indicates aerodynamically smooth conditions, such as a bay or a fallow field, and a large value indicates the presence of large obstructions, such as buildings or trees.

AFFILIATIONS: MASTERS AND BACON—Department of Civil and Coastal Engineering, University of Florida, Gainesville, Florida; VICKERY—Applied Research Associates, Raleigh, North Carolina; RAPPAPORT—NOAA/National Hurricane Center, Miami, Florida
CORRESPONDING AUTHOR: Forrest Masters, Assistant Professor, Department of Civil and Coastal Engineering, University of Florida, 365 Weil Hall, Gainesville, FL 32611
E-mail: masters@ce.ufl.edu

The abstract for this article can be found in this issue, following the table of contents.
DOI:10.1175/2010BAMS2942.1

In final form 25 June 2010

Using established wind speed conversion techniques, z_0 can be found from a known GF (Ashcroft 1994). In this study, effective z_0 values are computed for 16 wind sectors at 148 stations. The z_0 values are termed *effective* because i) most terrain surrounding airports is heterogeneous, and the formation of internal boundary layers is not presently considered; and ii) z_0 is determined from wind speed records collected at a single height because the vertical velocity profile is unknown.

The proposed method is robust, efficient, and easily updated when new research and/or data become available. The full dataset is accessible from the National Oceanic and Atmospheric Administration (NOAA) Hurricane Research Division's (HRD) Tropical Cyclone Wind Exposure Documentation Project (Powell et al. 2004; www.aoml.noaa.gov/hrd/asos), which maintains a public database of roughness lengths and displacement heights of ASOS in hurricane-prone areas that were determined using a visual technique. The research herein serves to augment this work.

The principal motivation for this research is to improve climatological and event-driven wind field analyses that are calibrated with surface wind field measurements. The z_0 value is a critical parameter in the boundary layer standardization scheme used to convert an in situ wind speed observation to an "equivalent" wind speed with a specified z, averaging duration t, and z_0. Collectively, z_0, z, and t are termed metadata (cf. Powell et al. 1996), and they vary by discipline. For example, the metadata widely used in structural design are the basic wind speeds found in ASCE-7 (2010). In operational hurricane forecasting, the Saffir–Simpson Hurricane Wind Scale (SSHWS) is used (Simpson 1974; Saffir 1975; www.nhc.noaa.gov/aboutsshs.shtml). Today, many modelers use aerial photographs or land use land cover information to assign directionally dependent z_0 values to surface weather observation sites, which are inherently subjective and deeply sensitive to the quality and age of photographs/database. In contrast, the proposed technique performs a mathematical analysis on historical wind speed records to estimate z_0 values.

The research also has the potential to aid users in hydrometeorology, climatology, and meteorology, which do not currently implement standardization schemes. It will be shown that direct usage of the raw data can introduce surface-layer gust speed errors on the order of 40%, which is consistent with the errors first observed by Powell et al. (1996). These errors can propagate into operational analysis and forecasts, model initialization, dynamic analysis, and verification. Numerical weather prediction, in particular, may benefit greatly as 3D and 4D assimilation into PBL modeling becomes more widely implemented. Thus, a secondary contribution of this paper is the determination of directionally dependent scalar multipliers to standardize raw mean wind speed data to 3-s gust and 1-h mean values at 10 m in flat, open terrain conditions.

This paper discusses airport terrain conditions and presents the methodology employed to estimate effective z_0 values from historical wind speed records. An effective z_0 database is offered. Potential improvements are addressed as a starting point for users to generate feedback for updating the database. Next, the results of the analysis are discussed in the context of terrain effects on wind speed observations. Lastly, an application of the database is presented using wind speed data collected in southeast Florida during Hurricane Wilma (2005).

AIRPORT TERRAIN CONDITIONS. The majority of AWOSs/ASOSs (hereafter ASOSs) are sited on airport grounds, which have layouts dominantly characterized by parallel, open V, and intersecting runways creating asymmetric patterns of flat, open terrain with large roughness elements interspersed (e.g., terminals, hangars, service buildings, parking garages, and stands of trees). The terrain immediately surrounding most ASOSs may be nominally characterized as aerodynamically very smooth. It consists of runway tarmacs (z_0 = 0.002–0.004 m; Bradley 1968), flat expanses of concrete (z_0 = 0.002–0.005 m; Sheppard 1947), and short grass (z_0 = 0.002–0.017 m; Deacon 1953). Terminals, concourses, hangars, service buildings, and stands of trees also share this space. Beyond the airport perimeter, a wide spectrum of terrain conditions is represented. Most airports are surrounded by built-up terrain that ranges from suburban neighborhoods to forests to metropolitan cities. This condition is idealized as a "rough to smooth" internal boundary layer (IBL) transition (Fig. 1a). Contrarily, some airports are located next to the ocean, the intracoastal waterways, or other large bodies of water. This configuration sets up a "smooth to rough" IBL transition (Fig. 1b) or a "smooth to rough to smooth" IBL transition (Fig. 1c) if a narrow patch of roughness separates the airport from the water body. For the purpose of this analysis, an effective roughness length value is determined (i.e., z_0 is directly estimated from the in situ measurements, which in almost all cases have spatially transitioning mean and turbulence intensities).

METHODOLOGY. The following subsections detail the procedure to estimate effective z_0 values from the ASOS data. Computation of wind speed conversion factors is also discussed. First, wind speed and sky condition data from the electronic archives at the National Climatic Data Center (NCDC) are acquired and merged. Second, data are checked for completeness and internal consistency, and those segments that meet both conditions undergo a five-step reduction process to isolate stationary, neutral equilibrium segments for analysis. GF values are computed from this reduced dataset, stratified into 16 wind sectors, and averaged to produce directional-mean GFs. Third, a crossing rate approach that accounts for gust-averaging duration, averaging type, and the effects of mechanical filtering is applied to convert mean GFs to effective z_0 values. This computation is dependent on instrument height and the station latitude, which are parameters in the mean wind speed and turbulence profile functions required to carry out this calculation. Last, wind speed conversion factors are computed for the purposes of wind field standardization and applied for the case of Hurricane Wilma (2005).

Data acquirement. Until recently, only hourly reports of ASOS surface wind observations were publicly available. These data possessed insufficient temporal resolution to reliably estimate z_0 values, and thus visual assessments were required. Continuous 1-min data archived at the NCDC became available in 2007. Data are available starting in 2000, although only a few years are available for the majority of stations. Approximately 27% of the stations in this study had full records, and 3-yr datasets were available for all of the stations.

The National Weather Service and the Federal Aviation Administration operate nearly 2,000 weather stations in the United States. Only the weather stations located in hurricane-prone areas are considered in the study, specifically ASOSs located <160 km from the coastline extending from Texas to New York (see Fig. 2). Observational data from two datasets were extracted for each station from the NCDC archives: DSI-6401 and DSI-6405. Five-min sky conditions—in the form of up to three altitude-specific cloud layers—detected by a ceilometer (see Table 1) are extracted from DSI-6401. Two-min moving-average and gust wind speeds and their corresponding directions, which are archived in 1-min intervals, are extracted from DSI-6405.

Quality control, data reduction, and synthesis. Once the sky condition and weather data are merged and

Fig. 1. Typical upwind terrain conditions surrounding an ASOS. Wind traveling from (right) west to (left) east over (a) rough-to-smooth transition, (b) smooth-to-rough transition, and (c) smooth-to-rough-to-smooth transition.

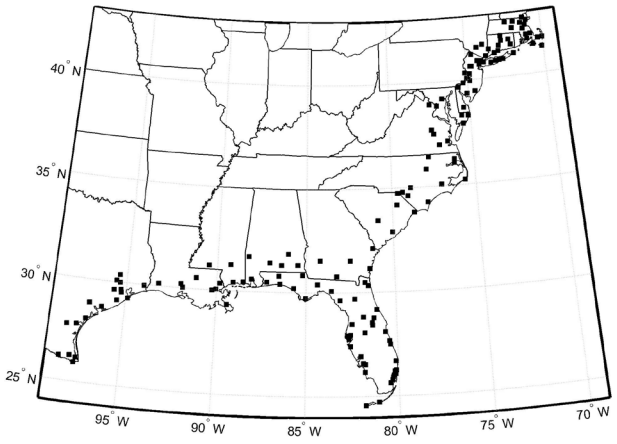

Fig. 2. Location of ASOSs that comprise the study set.

synchronized, the data are quality controlled and reduced. Given the sheer quantity of data, it was necessary to develop an automated approach to process the data efficiently. Figure 3 depicts the approach. The wind speed records (DSI-6405) are divided into 10-min contiguous segments within each hour, and each segment is processed separately. If any missing or irregular values or corrupted lines are found in the ten 1-min records within the segment, the program discards it and moves to the next segment. Segments with data deemed complete and within bounds are then subjected to five tests to cull nonstationary, stable, and/or unstable records. If any of the following criteria are met, the candidate segment is disqualified for inclusion in the analysis:

i) $U(600\ \text{s}) < 5\ \text{m s}^{-1}$. The mean wind speed is an average of every other five 2-min wind speed averages in the 10-min record, which contains 1-min entries.
ii) The wind direction is too variable based on either of the following two conditions:
a) The scalar and vector mean $U(600\ \text{s})$ values differ by $>0.51\ \text{m s}^{-1}$ (1 knot) or
b) The standard deviation of the wind direction >10° (calculated per Yamartino 1984).
iii) Noise or anomalous gust value(s) are detected, which are defined as $\hat{u} > 5$ standard deviations from the mean. This check is also intended to remove spurious reports caused by birds landing on the ultrasonic sensors (Schmitt 2009)
iv) The wind speed data are nonstationary (i.e., the statistical properties of the wind change within the record, thus affecting the ensemble moments). A reverse arrangement test is performed (see Bendat and Piersol 2000), and the hypothesis that the record is stationary is accepted at the $\alpha = 0.05$ level of significance
v) Nonneutral atmospheric conditions are present. Following the approach of Wieringa (1973), the Pasquill (1961) stability class is determined using the empirical stratification illustrated in Fig. 4. Although the GFs collected during stable and unstable conditions are not used in this study, they are stored for future analysis. Each record is classified as stable, unstable, or neutrally stratified based the following parameters:
a) $\bar{U}$ (3,600 s), determined by dividing $\bar{U}$ (600 s) by 1.075. This conversion factor is only strictly valid if the 10-min mean is the maximum within the hour. Thus, it is prone to removing records that would have been categorized as neutral if the true 1-h mean wind speed were known.
b) Diurnal cycle, based on the official zenith calculated according to Doggett (1990).
c) Season, as defined by meteorological reckoning.
d) The degree of cloud cover, which is found from the segment's corresponding two entries of 5-min sky condition values in the DSI-6401 archive. As many as three values from Table 1 may be reported in each 5-min record, but only the maximum cloud cover condition is selected (e.g., if the codes SCT, BKN, and OVC are present, then OVC is selected; acronyms defined in Table 1). The two sky condition codes are converted to a percentage of cloud cover and averaged (e.g., the average of SCT + OVC = 37.5%/2 + 93.5%/2 = 65.5%).

Table 1. Sky condition as reported by the ceilometers and the assumed percentage range of cloud cover.

Code	Sky condition	Cloud cover (%)	Cloud cover used in analysis (%)
CLR	Clear	0 to ≤5	2.5
FEW	Few	>5 to ≤25	15.0
SCT	Scattered	>25 to ≤50	37.5
BKN	Broken	>50 to ≤87	68.5
OVC	Overcast	>87 to 100	93.5

GF(600 s, t) values are calculated for all segments that are not disqualified and then are stratified by wind direction sectors (north, north-northeast, . . . , north-northwest) and anemometer type. The two instruments currently used by the ASOSs are the Belfort 2000 cup anemometer and Vaisala NWS 425 ultrasonic anemometer (NWS 2003). Averages are calculated for both instruments.

GF measurements collected from the same instrument in the same direction are known to vary widely from one record to the next, even when all other conditions appear to be the same. Thus, a large sample set was required to estimate the mean value. If at least $N = 30$ samples are available, then the values are averaged to determine the expected (mean) GF value:

$$\overline{GF}_j(600,t,z,z_0) = \frac{1}{N}\sum_N GF(600,t,z,z_0). \quad (2)$$

Given identical terrain and wind field conditions, the $\overline{GF}$ value computed from the Belfort anemometer is expected to be less than the $\overline{GF}$ value computed from the Vaisala, owing to their different gust-averaging durations, averaging methods, and frequency response characteristics. The Belfort reports a 5-s nonoverlapping block-average gust, and the Vaisala reports a 3-s moving-average gust. The Belfort anemometer is of the cup variety, and the Vaisala is an ultrasonic sensor. The Belfort has a distance constant (λ) of <10 m, where λ is defined as the length of the airflow required to pass the anemometer before the cups register a 63.2% step change. The Vaisala ultrasonic anemometer uses sound to measure velocity. For practical purposes, its distance constant is considered to be zero.

The combined effect of averaging duration, averaging type, and mechanical filtering acts to attenuate the measurement of the peak gust of the Belfort relative to the Vaisala. It is visually discernable in multiyear datasets. Consider the 9-yr record of neutrally stratified GF data collected from the south-southeast sector of Pensacola Regional Airport (KPNS, Florida) shown in Fig. 5. When the Belfort was replaced with a Vaisala in March 2007, the 10-min $\overline{GF}$ abruptly shifted from 1.32 to 1.41 (+7%). Similar trends were observed at the remaining stations equipped with ultrasonic anemometers.

Development of gust factor–z_0 relationships. A theoretical GF model was applied to estimate directionally dependent z_0 values for the two anemometer systems:

$$\overline{GF}(T,t,z,z_0) = 1 + g(T,t,z)\frac{\sigma(T,t,z,z_0)}{U(z,z_0)}, \quad (3)$$

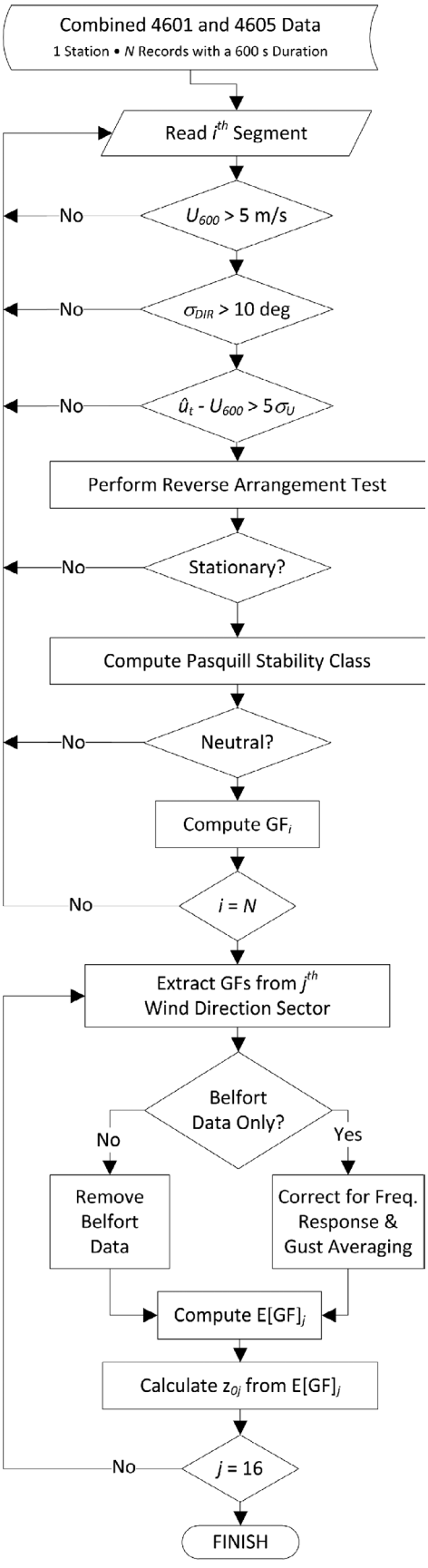

Fig. 3. Data reduction algorithm.

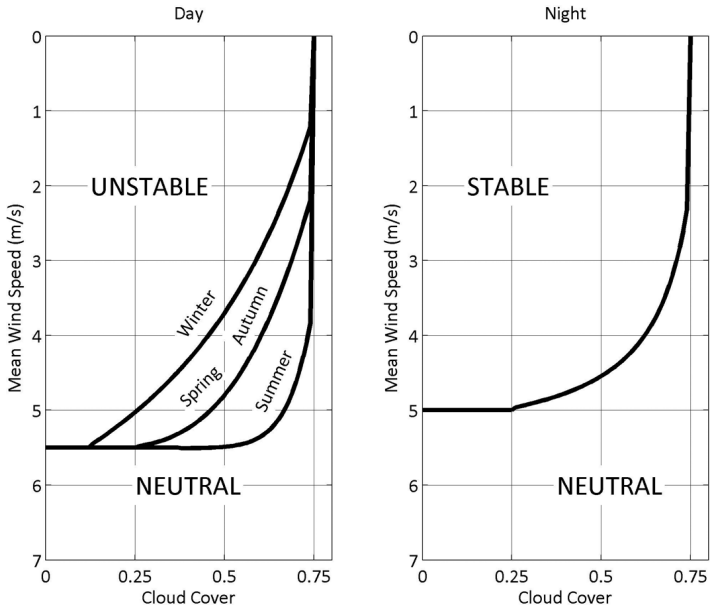

Fig. 4. Pasquill stability stratification (after Wieringa 1973).

where $g(T, t, z)$ is a peak factor and $\sigma(T, t, z, z_0)$ is the standard deviation of the fluctuating component of the wind. Note that both $g(T, t, z)$ and $\sigma(T, t, z, z_0)$ depend on t and T. The peak factor is influenced by the response time of the wind-measuring system through a reduction in the upcrossing frequency (Davenport 1964):

$$g(T,t,z) = \sqrt{2\ln(\nu T)} + 0.577/\sqrt{2\ln(\nu T)}, \quad (4)$$

where ν is the cycling rate computed from

$$\nu^2 = \frac{\int_0^\infty f^2 S(f,z,z_0)\chi^2(f)df}{\int_0^\infty S(f,z,z_0)\chi^2(f)df}. \quad (5)$$

Here $S(f, z, z_0)$ is the one-sided power spectral density of longitudinal turbulence, which, in this study, is of the von Kármán form found in Greenway (1979):

$$\frac{fS(f)}{\sigma_u^2} = \frac{4f\dfrac{L_u^x}{\overline{U}}}{\left[1+70.8\left(f\dfrac{L_u^x}{\overline{U}}\right)^2\right]^{5/6}}; \quad (6)$$

$S(f, z, z_0)$ is dependent on the integral length scale of the wind, L_u^x, and the variance of the longitudinal component of the wind, σ_u^2. Other forms of the longitudinal wind spectra can be substituted (e.g, Kaimal et al. 1972; Tieleman 1995), but variations in the spectra shape were found to have very little influence on the GF calculation. The GF is sensitive to the σ_u^2 term, which is dependent on z_0. In this study, the modified form of the Harris and Deaves (1981) variance model given in ESDU (1983) and described in Vickery and Skerjl (2005) was used:

$$\sigma_u = \frac{u_* 7.5\eta[0.538+0.09\ln(z/z_0)]^{\eta^{16}}}{1+0.156\ln(u_*/fz_0)}, \quad (7)$$

which is dependent on the friction velocity u_* and the scaling parameter

$$\eta = 1 - 6fz/u_*. \quad (8)$$

The filter $\chi^2(f)$ in Eq. (5) takes into account the data acquisition and processing (sample frequency, averaging time, and averaging method) and the frequency response characteristics of the anemometer (cf. Beljaars 1987). In the case of the Vaisala anemometer, which has no moving parts and computes the peak gust from an overlapping moving average, the filter function is simply

$$\chi^2(f) = \left[\frac{\sin(\pi ft)}{\pi ft}\right]^2 - \left[\frac{\sin(\pi fT)}{\pi fT}\right]^2. \quad (9)$$

The first filter term accounts for the short-duration averaging of the data. The second term accounts for the low-frequency energy that is not captured when the record duration is shorter than 30–60 min. The Belfort system, which is a mechanical instrument that computes

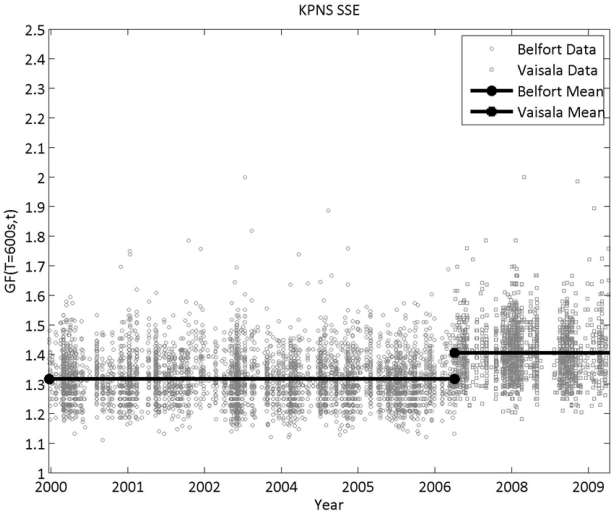

Fig. 5. Record of neutral stability gust factors collected at KPNS. The Belfort three-cup anemometer was replaced on 27 Mar 2007 with a Vaisala ultrasonic anemometer.

the peak gust from a nonoverlapping block average, is characterized by a three-component filter chain,

$$\chi^2(f) = \left[\frac{\sin(\pi f t)}{\pi f t}\right]^2 \cdot \frac{1}{N^2}\left[\frac{\sin(\pi f \Delta N)}{\sin(\pi f \Delta)}\right]^2 \cdot \frac{1}{1+\left(\frac{2\pi n\lambda}{U}\right)^2}, \quad (10)$$

where t is the duration of the nonoverlapping block average, δ is the time interval between samples, and N is the number of samples in the average. The product of the first and second terms represents the filter associated with a nonoverlapping block (segmental) average (Beljaars 1987; Miller 2007). The last term represents the linear filter that accounts for the mechanical filtering of the cup anemometer. It is dependent on λ and the mean wind speed at the anemometer (Greenway 1979).

From Eqs. (3)–(10), it is clear that the gust-averaging technique, gust duration, and anemometer distance constant affect the GF through both a reduction in the measured standard deviation and the number of standard deviations the gust is away from the mean. Figure 6 compares the GF curves for the Vaisala and Belfort systems for a mean wind speed of 10 m s^{-1} at an elevation of 10 m. The difference between the Vaisala and Belfort GF values monotonically increases from 3% to 11% over the range of roughness lengths shown. The implication is that the Vaisala anemometers are expected to report "gustier" winds than the Belfort anemometers in day-to-day weather conditions.

Figure 7 contains data from a subset of ASOS stations in this study that replaced the cup anemometer with the ultrasonic sensor during the archival period. Directionally dependent effective z_0 values computed from both eras of sensors are plotted in coordinate pairs (Vaisala versus Belfort) to evaluate the consistency and robustness of the theoretical treatment. In both plots, the vertical coordinates are the same effective z_0 values computed from the Vaisala sensor. In the left panel, the abscissas are computed from

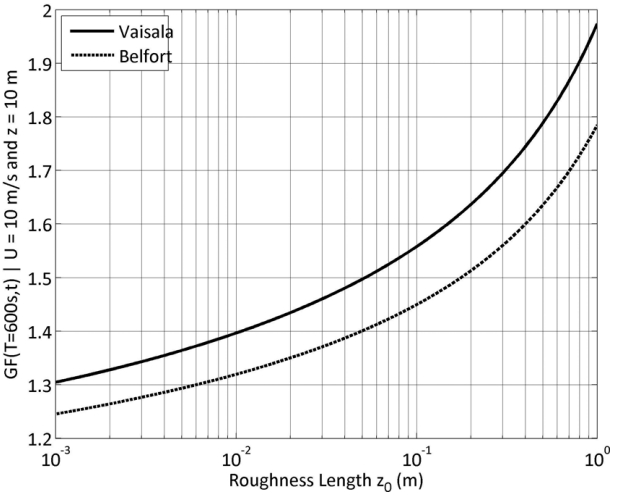

Fig. 6. GF values for the Vaisala and Belfort systems derived from a crossing rate approach.

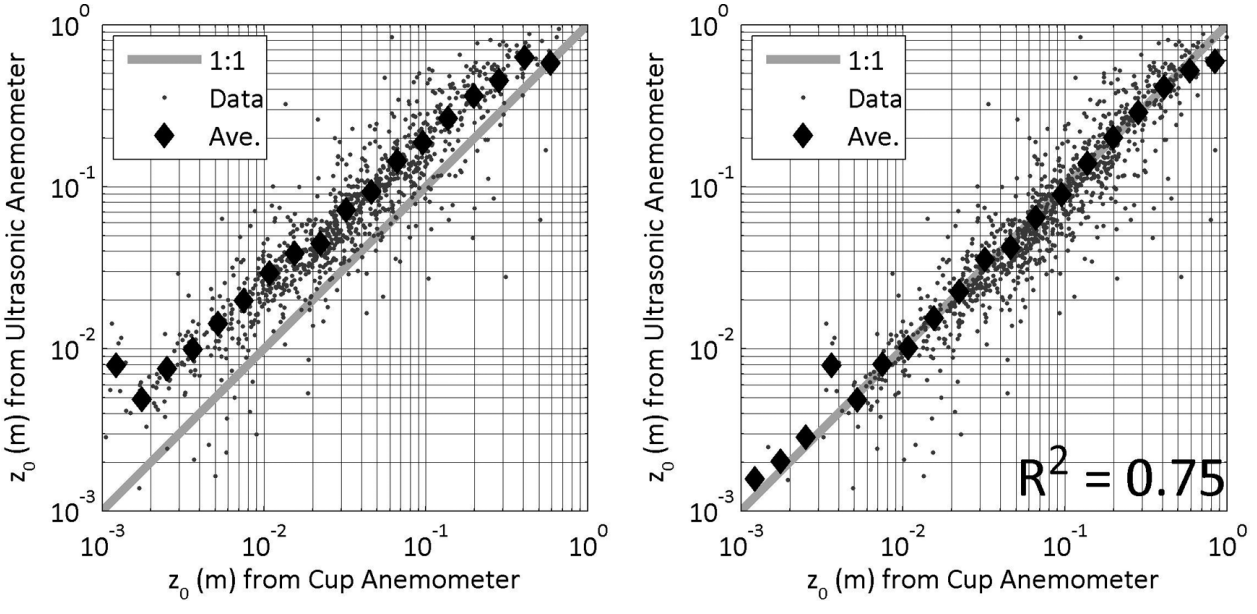

Fig. 7. Comparison of effective z_0 values computed using the Belfort and Vaisala data collected during different eras. Each point represents a single direction from one airport. (left) The results without consideration of block averaging and instrument response. (right) Once the Belfort data are correctly filtered, they compare favorably to measurements from the Vaisala.

Belfort data without block averaging and instrument filters being applied. Only 5-s averaging is considered using Eq. (9). Thus, the effects of the data processing and anemometer response are seen; however, the effect of different averaging times of the two instruments are not. The abscissas in the right panel are the effective z_0 values computed from the filter chain in Eq. (10). For reference, both plots contain a thick gray line with a slope of unity (1:1). Binned averages of the data are depicted by the diamond markers.

A bias is clearly seen in the uncorrected data (left panel). Very good agreement is seen in the corrected data (right panel). Fitting the 1:1 line to the data yields a coefficient of determination (R^2) of 0.75, which demonstrates that the theoretical correction works well over a wide range of terrain conditions.

Computation of conversion factors for wind field standardization. Boundary layer or wind field "standardization" methods are applied to convert raw wind speed measurements to a common set of metadata (i.e., z_0, z, t). A 10-m height is practically universal, but the choice of duration and terrain is mostly discipline specific. For example, the standard metadata for most wind engineering applications are $z_0 = 0.03$ m and $t = 3$ s, while the storm surge modeling community generally uses a 10-min average in marine conditions.

The standardization process is now generalized for conversion of a gust observation to the equivalent value for a specified set of metadata. The reader is referred to Vickery and Skerlj (2005) for more information. The gust observation is divided by $\overline{GF}$ [determined from Eq. (3)] to calculate the hourly mean. The z_0 value must be known or assumed to perform this calculation. Next, u_* is computed from the logarithmic law. It is constant through the surface layer and therefore height independent. Then, u_* is converted to its equivalent value in the standardized conditions, and the new mean wind speed is computed with the logarithmic law. Alternatively, the conversion can be performed directly on the mean wind speed or velocity pressure with the height considered (see Irwin 2006). In the last step, the mean wind speed is multiplied by the gust factor computed from Eq. (3) to calculate the standardized gust speed. If the upwind terrain at the observation site or the desired metadata corresponds to over water conditions, then the corresponding z_0 value must be found using an iterative scheme that employs a drag coefficient model to relate the marine roughness to the mean wind speed (e.g., Large and Pond 1981; assuming shallow water conditions can be reasonably represented by a deep-water model). An upper bound on the drag coefficient should be applied to account for the leveling off of drag at high wind speeds, which is a phenomenon observed in surface wind speed measurements in hurricanes (Powell et al. 2003; Uhlhorn et al. 2007)

Limitations of the approach (opportunities for improvement). The intent of this study was to produce an efficient, automated framework to quantify mean gust factors occurring in neutral stability conditions to estimate effective z_0 values. Updates to the data stratification and analysis models are planned. Working with a finite amount of data and resources, it was not possible in this round of research to implement the following advanced stratification techniques:

i) It is speculated that thunderstorms have larger GFs than extratropical and tropical wind events (Choi and Hidayat 2002; Orwig and Schroeder 2007; Lombardo et al. 2009). Although the algorithm did not explicitly target these events for removal, it is highly probable that the data reduction measures that were implemented (e.g., removing records with large peak-to-mean ratios and nonstationary trends) indirectly acted to remove most thunderstorm activity. We do note that applying standard boundary layer theory in the theoretical adjustment of the 5-s block-average gusts to the 3-s moving-average gusts computed works quite well with the wind data used here, irrespective of storm type.
ii) Given the low threshold of wind speeds, the rate of momentum exchange over bodies of water was not fully realized in the data. It is recognized that the surface drag increases with wind speed until it levels off when the wind speed approaches SSHS category 1 conditions (Powell et al. 2003). In wind sectors containing water, the z_0 values are expected to increase proportionally to the wind speed. A drag coefficient model can be employed to estimate an upper z_0 bound for wind speeds less than 35–40 m s^{-1}.
iii) Seasonal variations were not considered. A small subset of the airports is sited next to crops and deciduous forests, which are subject to interannual variations in the vegetation density.
iv) The estimation technique is expected to be more accurate for flat, open terrain than in dense suburban or city landscapes. An exact upper z_0 bound is not known, but Wieringa (1973) has shown that roughness lengths derived from gust factors at 10 m can be estimated when $z_0 < \sim 0.40$ m.
v) The $\overline{GF}$ was considered to be invariant with wind speed, while in the strict sense, the longitudinal

turbulence component is not due to its dependency on the Rossby number (Harris and Deaves 1981). The result is that $\overline{GF}$ is expected to decrease slightly with increasing wind speed (Ashcroft 1994). The literature has widely applied this assumption, and it is considered to be valid in this analysis because the range of shear velocity estimates is confined to a relatively small range.

vi) This approach does not presently consider nonlinear cup anemometer dynamics (i.e. overspeeding), which will introduce errors in the mean wind speed that are <2% (per Busch and Kristensen 1976).

RESULTS. A large database of surface wind field measurements was analyzed at 148 ASOS stations to characterize directionally dependent z_0 values from $\overline{GF}$ values. Stratifying the data to remove stable and unstable conditions reduced the dataset by 33% when the mean wind speed threshold was set to 5 m s^{-1}. After records with first-order nonstationary trends, large shifts in direction, and anomalous gusts were removed, the rejection rate increased to nearly 42%.

After the data reduction, more than seven million 10-min segments spanning nine years from nearly 2,400 unique terrain sectors remained. The directional $\overline{GF}$ values range is [1.21, 2.00] for the Belfort anemometer and is [1.23, 2.18] for the Vaisala anemometer. A review of the aerial imagery indicates that the use of ASOS wind speed data appears to be an excellent tool to distinguish the "signature" of upwind terrain. Figure 8 contains the probability distribution function (PDF) and the cumulative distribution function (CDF) of the estimated effective z_0 values. Assuming open exposure is defined as 0.02 m ≤ z_0 < 0.07 m, 34% of the ASOS wind sectors in the study set qualify as open exposure conditions; 16% have z_0 values less than 0.02 m; and 50% have z_0 values greater than 0.07 m.

Users of the z_0 estimates published herein should always compare these values to other estimates before an engineering/meteorological judgment is made. The true local roughness is not known in the absence of neutral wind speed profile data above the site in question. No particular method—anemometric, morphometric, visual, or otherwise—can be correctly described as the "standard" approach to estimating z_0 values (Grimmond et al. 1998).

Figure 9 contains the PDF and CDF for the wind speed multipliers to convert the gust speed measured by the Belfort cup anemometer to an equivalent ASCE-7-10 basic wind speed (t = 3 s; z = 10 m; z_0 = 0.03 m). Figure 10 contains the PDF and CDF for the wind speed multipliers to convert the 1-h wind speed average to an equivalent 1-h open exposure average (T = 3,600 s; z = 10 m; z_0 = 0.03 m). In both cases, the majority of the wind speed multipliers are larger than unity, which indicates that direct usage of ASOS wind data is expected to underestimate open exposure surface wind field intensity.

The entire database was also compared to visual estimates recorded in the NOAA Hurricane Research Division's Tropical Cyclone Wind Exposure Documentation Project (Powell et al. 2004). Figure 11 contains a plot of the GF-derived z_0 estimates and the published z_0 estimates available on the HRD Web site. The hollow square boxes are averages of the GF-derived estimates. Although the mean values of the estimated effective z_0 values are similar, the scatter is quite large, and there exists a tendency for the analyst on the ground to assume an open exposure when the immediate open exposure fetch is large. The average visual estimate improves for more built-up conditions, as a lower limit of 0.03 m was assumed in the Powell et al. (2004) study. Assuming the objective

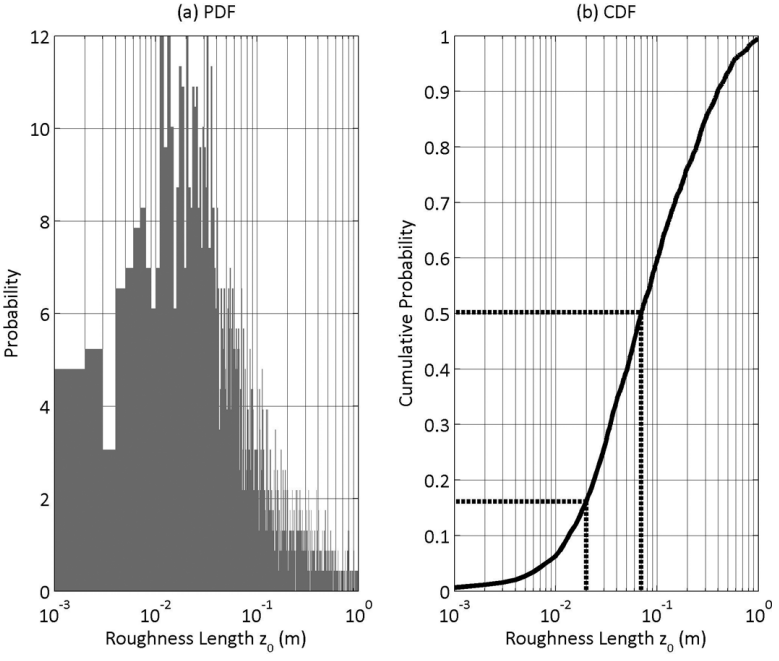

Fig. 8. The (a) PDF and (b) CDF of the roughness length estimates for 148 study stations. The dashed lines in (b) are the bound open exposure terrain conditions (0.02 m < z_0 < 0.07 m).

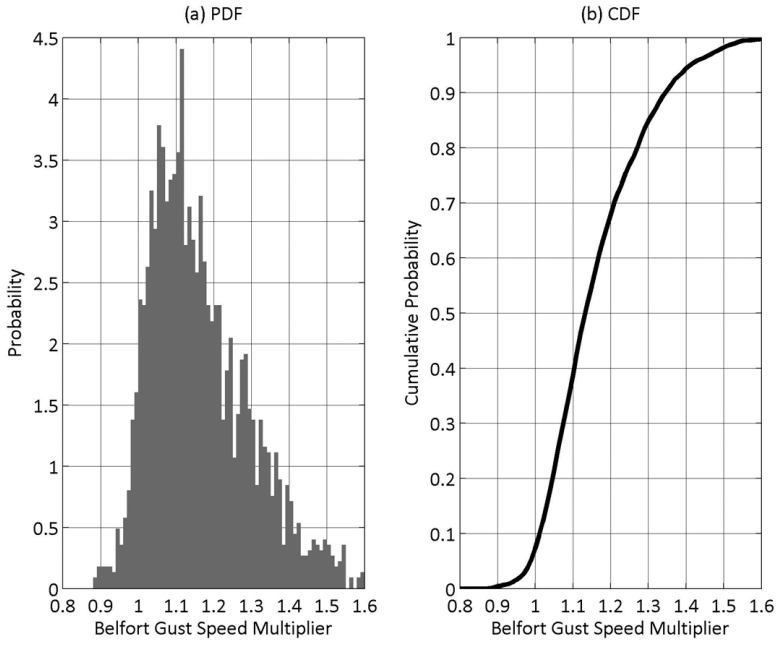

Fig. 9. Distribution of multipliers to convert Belfort gust values to an open exposure 3-s equivalent value.

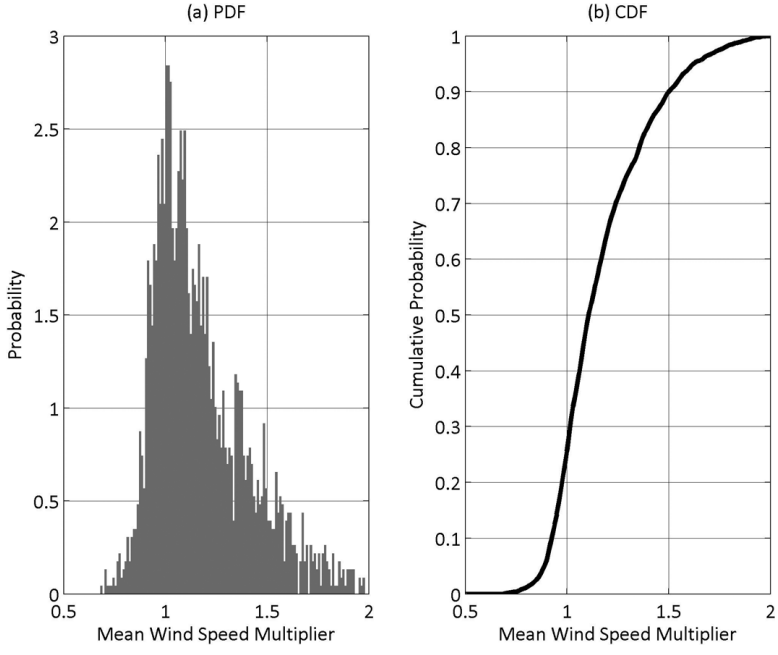

Fig. 10. Distribution of multipliers to convert 1-h mean wind speed values to an open exposure 1-h mean wind speed value.

estimates provide a reasonable baseline for roughness length estimation, it can be inferred that examination from the ground is usually insufficient to characterize the local roughness length.

The results from a subset of stations are now discussed. Table 2 contains effective z_0 estimates for 10 airports: Key West International (KEYW), Florida; Mobile Regional (KMOB), Alabama; KPNS and Tampa International (KTPA), Florida; William P. Hobby (KHOU) and Pearland Regional (KLVJ), Texas; Lakefront (KNEW) and Louis Armstrong International (KMSY), Louisiana; and Miami International (KMIA) and Opa-Locka Executive (KOPF), Florida. Wind direction sectors containing marine conditions within 2 km upwind of the site have shaded cells. The GF values were measured in very low wind speeds, and at least for ocean exposure upwind, are expected to increase with wind speed because the drag coefficient over water is velocity dependent. For bays and estuary systems, the z_0 estimates may be appropriate for all wind speeds, but this condition must be assessed case by case. For practical purposes, the values listed in the shaded cells may be assumed as being the lower z_0 bound. A capped drag coefficient model can be employed to determine an upper z_0 bound, when required.

The results clearly indicate that airports have diverse upwind terrain conditions. Variations in z_0 estimates are as large as one order of magnitude. Open exposure conditions are predominant, but half of the airports have at least one direction sector that is classifiable as built-up terrain ($z_0 > 0.15$ m). Differences between the results for airports collocated in the same region [KHOU–KLVJ; KNEW–KMSY; KMIA–KOPF; and John F. Kennedy International Airport (KJFK)–La Guardia Airport (KLGA), New York] are also noted. The implication is significant for the use of land-based weather station data to monitor local weather conditions. If the upwind terrain conditions vary significantly at an airport (or between airports), then variations in the wind field intensity may be incorrectly attributed to the structure of the local weather system, or possibly "background" observational noise, when the terrain variability is actually the cause.

Table 3 contains the wind speed multipliers to convert the gust speed measured by the Belfort cup anemometer to an equivalent ASCE-7-10 basic wind

speed, which is a 3-s moving-average gust measured at 10 m in flat, open country. Table 4 contains the corresponding multipliers for the stations that were recently upgraded to the Vaisala ultrasonic anemometer.

The gust wind speed multipliers are found to be as large as 1.42, which implies that the true open exposure gust is expected to be ~40% larger than the measured value. This result is in good agreement with the "consequence" errors in the standardization process first noted by Powell et al. (1996). We note that in the case of wind loads on buildings, errors in the wind speed estimates are at a minimum squared when converted to wind loads; in the case of wind power, the errors are cubed.

Table 5 contains the multipliers to convert the 1-h wind speed average to an equivalent 1-h open exposure average, which is based on a conversion of the 2-min wind speed average. The vast majority of ASOS data are stored in Aviation Routine Weather Reports (METAR) recorded hourly, which contain the last recorded 2-min wind speed average. These short-duration averages can be treated as samples of a process that is treated as nominally stationary over a period of about an hour or so [the period approximately represented by the spec-

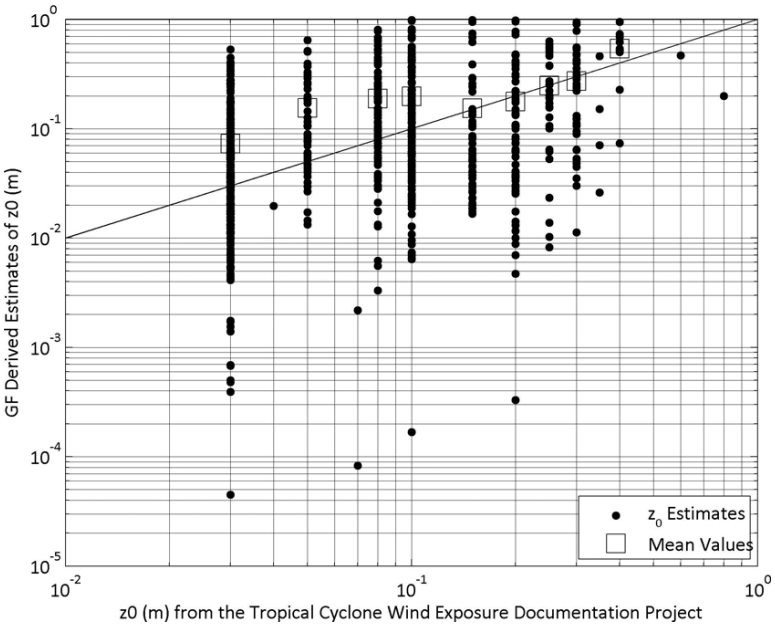

Fig. 11. Comparison of objective z_0 estimates to the visual estimates archived in the Tropical Cyclone Wind Exposure Documentation Project.

Table 2. Directional effective roughness length estimates for selected airports. Shaded cells indicate that the upwind terrain has marine exposure. The user should perform appropriate adjustments for wind speed. Italicized values indicate z_0 > 0.4 m. As the roughness length grows larger, the accuracy of the method is expected to decrease.

	KEYW	KMOB	KTPA	KPNS	KHOU	KLVJ	KMIA	KOPF	KMSY	KNEW
N	0.0041	0.0362	0.0542	0.0917	0.0280	0.0709	*0.4019*	0.0426	0.0209	0.0003
NNE	0.0030	0.0255	0.1121	0.1396	0.0211	0.0681	0.3037	0.0370	0.0069	0.0001
NE	0.0023	0.0359	0.1857	*0.4071*	0.0207	0.0635	0.1164	0.0292	0.0117	0.0001
ENE	0.0085	0.0386	0.3611	*0.5325*	0.0656	0.0708	0.0648	0.0154	0.0515	0.0001
E	0.0148	0.0377	0.3988	0.1856	0.1881	0.0735	0.0111	0.0166	0.1228	0.0022
ESE	0.0021	0.0136	0.3659	0.0343	0.1553	0.0855	0.0188	0.0177	0.1013	0.0052
SE	0.0014	0.0189	0.3228	0.0153	0.2608	0.0931	0.0714	0.0130	0.0487	0.0077
SSE	0.0016	0.0270	0.2629	0.0114	0.2082	0.1440	0.1234	0.0110	0.0200	0.0074
S	0.0050	0.0380	0.1421	0.0111	0.1916	0.1801	0.1195	0.0230	0.0100	0.0045
SSW	0.0053	0.0434	0.0868	0.0188	0.1039	0.2623	0.0994	0.0279	0.0263	0.0036
SW	0.0026	0.1001	0.0464	0.0248	0.0556	*0.4065*	0.1052	0.0242	0.0213	0.0017
WSW	0.0403	0.2651	0.0188	0.0415	0.0473	0.2650	0.0899	0.0255	0.0183	0.0005
W	0.0272	0.2467	0.0202	0.0463	0.0644	0.3043	0.1731	0.0338	0.0088	0.0000
WNW	0.0166	0.2279	0.0738	0.0481	0.1043	0.2700	0.2342	0.0303	0.0146	0.0001
NW	0.0037	0.1513	0.0814	0.0383	0.0903	0.1998	0.3226	0.0305	0.0336	0.0002
NNW	0.0024	0.0417	0.0562	0.0337	0.0455	0.1314	0.2490	0.0430	0.0341	0.0002

Table 3. Directionally dependent multipliers to convert gust speed measured by the Belfort cup anemometer to an equivalent ASCE-7-05 basic wind speed (t = 3 s; z = 10 m; z_0 = 0.03 m). Factors include both effects of terrain and differences between gust measurement and averaging times between the Belfort and ASOS systems. Belfort data were not available for KNEW. See Table 4 to convert Vaisala data.

	KEYW	KMOB	KTPA	KPNS	KHOU	KLVJ	KMIA	KOPF	KMSY
N	1.03	1.11	1.14	1.20	1.05	1.17	1.34	1.08	1.09
NNE	1.04	1.05	1.22	1.22	1.03	1.17	1.30	1.07	1.00
NE	1.01	1.06	1.29	1.39	1.03	1.16	1.17	1.06	1.02
ENE	1.09	1.08	1.40	1.36	1.12	1.17	1.12	1.02	1.11
E	1.10	1.05	1.42	1.15	1.23	1.17	1.00	1.02	1.20
ESE	0.99	1.01	1.40	1.03	1.21	1.19	1.03	1.02	1.17
SE	0.96	1.03	1.38	1.02	1.27	1.20	1.13	1.01	1.10
SSE	1.01	1.05	1.34	0.99	1.24	1.25	1.18	1.00	1.05
S	1.02	1.09	1.25	1.01	1.23	1.28	1.18	1.04	1.01
SSW	1.08	1.07	1.19	1.03	1.16	1.34	1.16	1.05	1.04
SW	1.00	1.13	1.13	1.05	1.10	1.42	1.16	1.04	1.05
WSW	1.12	1.25	1.06	1.10	1.09	1.34	1.15	1.05	1.03
W	1.24	1.25	1.07	1.12	1.12	1.37	1.22	1.07	1.02
WNW	1.15	1.24	1.18	1.13	1.16	1.35	1.26	1.06	1.04
NW	1.01	1.20	1.19	1.08	1.15	1.30	1.31	1.06	1.07
NNW	0.97	1.11	1.15	1.12	1.09	1.24	1.27	1.08	1.11

Table 4. Directionally dependent multipliers to convert gust speed measured by the Vaisala ultrasonic anemometer to an equivalent ASCE-7-05 basic wind speed (t = 3 s; z = 10 m; z_0 = 0.03 m). Multipliers due to terrain effects only.

	KEYW	KMOB	KPNS	KMSY	KNEW
N	0.91	1.01	1.08	0.98	0.85
NNE	0.90	0.99	1.12	0.93	0.83
NE	0.89	1.01	1.25	0.95	0.82
ENE	0.94	1.02	1.29	1.04	0.83
E	0.96	1.01	1.15	1.11	0.91
ESE	0.88	0.96	1.01	1.09	0.94
SE	0.87	0.97	0.96	1.03	0.96
SSE	0.88	0.99	0.95	0.98	0.96
S	0.91	1.01	0.95	0.94	0.93
SSW	0.92	1.02	0.97	0.99	0.93
SW	0.89	1.09	0.99	0.98	0.90
WSW	1.02	1.19	1.02	0.97	0.86
W	0.99	1.18	1.03	0.94	0.81
WNW	0.97	1.17	1.03	0.96	0.82
NW	0.90	1.13	1.02	1.01	0.84
NNW	0.89	1.02	1.01	1.01	0.84

Table 5. Directionally dependent multipliers to convert an observed T = 1-h wind speed to a 10-m, open exposure value.

	KEYW	KMOB	KTPA	KPNS	KHOU	KLVJ	KMIA	KOPF	KMSY	KNEW
N	0.84	1.02	1.12	1.15	0.99	1.16	1.50	1.04	0.96	0.75
NNE	0.83	0.98	1.24	1.22	0.96	1.15	1.41	1.02	0.88	0.71
NE	0.81	1.02	1.36	1.50	0.96	1.14	1.19	1.00	0.91	0.70
ENE	0.89	1.03	1.56	1.60	1.10	1.16	1.09	0.94	1.06	0.71
E	0.93	1.02	1.60	1.28	1.28	1.16	0.91	0.94	1.20	0.83
ESE	0.81	0.93	1.57	1.01	1.24	1.19	0.95	0.95	1.16	0.88
SE	0.79	0.95	1.52	0.94	1.36	1.21	1.11	0.92	1.06	0.91
SSE	0.80	0.99	1.46	0.91	1.31	1.29	1.20	0.91	0.96	0.91
S	0.86	1.03	1.29	0.91	1.29	1.35	1.19	0.97	0.90	0.87
SSW	0.86	1.04	1.19	0.95	1.17	1.45	1.16	0.99	0.99	0.86
SW	0.82	1.16	1.10	0.98	1.07	1.61	1.17	0.98	0.97	0.82
WSW	1.03	1.37	0.99	1.04	1.05	1.46	1.14	0.98	0.95	0.76
W	0.99	1.35	1.00	1.05	1.09	1.50	1.26	1.01	0.89	0.69
WNW	0.94	1.33	1.17	1.05	1.17	1.46	1.34	1.00	0.93	0.70
NW	0.84	1.24	1.18	1.03	1.14	1.38	1.42	1.00	1.01	0.73
NNW	0.81	1.04	1.12	1.01	1.05	1.27	1.35	1.04	1.01	0.73

tral gap as indicated in, for example, the van der Hoven (1957) spectrum]. Since the sampled winds are not maxima, but are simply random samples of a process considered to be stationary for about an hour, the statistics derived from that data are representative of winds having a mean averaging time of about an hour. Consequently, the terrain corrections that are applied to these 2-min samples are those computed for the mean winds. It is noteworthy that these mean wind speeds are much more sensitive to terrain corrections than the gust wind speeds (compare Tables 3 and 5). The range of wind speed multipliers is [0.69, 1.61], which is much larger than the gust cases. All other factors being equal, short-duration peak gusts measured in different terrains are expected to compare more favorably than longer-duration averages measured in the same conditions.

These data can be used for the development of directional wind climate models for use in conjunction with wind tunnel test data for the design of buildings (e.g., Davenport 1983; Lepage and Irwin 1985). Similarly, the hourly mean wind speed corrections should be applied to the data when used for developing wind statistics for wind energy siting.

APPLICATION: CHARACTERIZATION OF HURRICANE SURFACE FIELD WIND INTENSITY. Meteorologists and engineers must assess the wind speeds in a landfalling tropical cyclone. Historically, a great deal of confusion has resulted because the two professions use different metadata to describe wind speeds.

In structural design and forensic engineering, the standard value is a peak 3-s gust speed at 10 m in open exposure conditions. U.S. building codes use a standard gust speed (or "basic wind speed") to calculate the freestream gust velocity pressure at 10 m. The basic wind speed is obtained from a wind speed map given in ASCE-7 (2010). This basic wind speed is converted to a pressure that acts on the surface of building. It is during this *pressure* conversion that the site-specific boundary layer effects (surface roughness, height, and topographic effects) are considered.

In operational meteorology, however, forecasters almost exclusively relay the intensity of a tropical cyclone to the general public in terms of the estimated maximum surface wind speed and the associated SSHWS category. It is defined as the 10-m, 60-s maximum surface wind speed that occurs in the storm domain, which, depending on the wind-induced sea state, is ~10% less than its ASCE-7 gust counterpart (Simiu et al. 2007).

Both metadata formats are necessary; one cannot be eliminated in favor of the other. Ideally, a straightforward conversion technique that can be implemented by operational forecasters for use by all audiences is needed. Tables 3 and 4 were developed

for this purpose, and are applied to convert wind speed records from Fort Lauderdale/Hollywood International Airport (KFLL), KMIA, and Palm Beach International Airport (KPBI), Florida, collected during the passage of Hurricane Wilma in 2005. A summary of the raw and standardized peak wind speeds are provided in Table 6.

Hurricane Wilma's center made landfall near Cape Romano, Florida, around 1030 UTC 24 October 2005, with associated maximum 1-min winds estimated by the National Hurricane Center (NHC) as 54 m s^{-1}. It traveled across the southern Florida peninsula and emerged into the Atlantic Ocean just southeast of Jupiter, Florida, around 1500 UTC, with 1-min wind estimated by the NHC as near 49 m s^{-1} (Beven et al. 2008).

Figure 12a contains the best track for Hurricane Wilma and the locations of the study ASOS stations. Figures 12b–d contain site-specific wind speed and direction time histories as well as the z_0 used to convert the observed gust speed to its 1-min marine and ASCE-7 equivalents (note that the equivalent 1-min value over land can be calculated by dividing the ASCE-7 3-s gust value by 1.27).

In the top plots of Figs. 12b–d, the gray lines correspond to the raw 5-s peak wind speed measured from the Belfort. The 1-min marine wind speed (using the z_0 values in Table 2) and the ASCE-7 basic wind speed (using the Belfort conversion factors in Table 3) are depicted by the thick black and red lines, respectively. The bottom plots in the subfigures contain 10-min averages of wind direction and the corresponding z_0 values found in Table 2. A velocity-dependent drag coefficient adjustment was not made to the z_0 values because at least 4 km separates the ASOS stations from open water.

Two eras of nominal design wind speeds are also included. The lower threshold corresponds to the local 50-yr recurrence interval design wind speed as required by American National Standards Institute (ANSI) A58.1 during 1982–93 (Mehta 1984). The upper threshold corresponds to the nominal design wind speeds that went into effect after the 1998 version of ASCE-7 wind load provisions were adopted.

An analysis of the standardized wind speeds is now discussed. First, the largest measured 2-min and 5-s wind speeds at KMIA were 30.9 and 41.2 m s^{-1}, respectively. Converting the gust report to a 1-min speed and making the correction for instrument response and roughness characteristics yields a 1-min marine wind speed equivalent value to 43.8 m s^{-1} (Table 6), which is consistent with the NHC's analysis of Hurricane Wilma's intensity as then a category 2 on the SSHS and with estimates from HRD H*Wind Analyses (found at www.aoml.noaa.gov/hrd; Powell et al. 1998). The table shows similar results obtained for KFLL and KPBI. Note that conversions performed using the peak 2-min mean value recorded by the ASOSs (not shown) produced similar results.

Second, the effect of wind field standardization is a reduction in the variability between collocated observations (Powell et al. 1996). This is noted here. Prior to standardization, the spread in the gust speeds is 4.1 m s^{-1}. Standardization reduces the spread to 2.4 m s^{-1}.

Third, the timing and direction of the peak wind speed can be determined and related to surrounding areas of varying exposure. While the raw data would support the general observation that the most intense wind speeds occur in the front right quadrant of a hurricane, after standardization it is seen, for Wilma over the southeastern peninsula, the data suggest the highest wind speeds occurred at the rear quadrant of the storm at KFLL and KPBI.

Fourth, it can be shown that neither current nor the previous nominal national design wind speed requirements were exceeded in the areas surrounding the airports. Thus, damage in the region can be attributed to one or more nonweather-related issues, such as inadequate provisioning in the building code, material age effects, installation errors, and/or underperforming building systems.

CONCLUSIONS. In this study, directional effective z_0 values were calculated from averages of neutrally stratified mean gust factors. A public domain database was created to assist wind field

Table 6. Peak wind speed observations at KFLL, KMIA, and KPBI during Hurricane Wilma.

	Measured peak 2 min			Measured peak gust			Gust used in conversion			1-min marine	3-s open
	U (m s^{-1})	θ (°)	z_0 (m)	U (m s^{-1})	θ (°)	z_0 (m)	u (m s^{-1})	θ (°)	z_0 (m)	u (m s^{-1})	u (m s^{-1})
KFLL	33.4	258	0.116	44.2	143	0.020	42.7	255	0.116	45.2	50.1
KMIA	30.9	153	0.123	41.2	151	0.123	41.2	154	0.123	43.8	48.6
KPBI	37.0	128	0.008	45.3	134	0.008	44.8	294	0.034	43.2	47.7

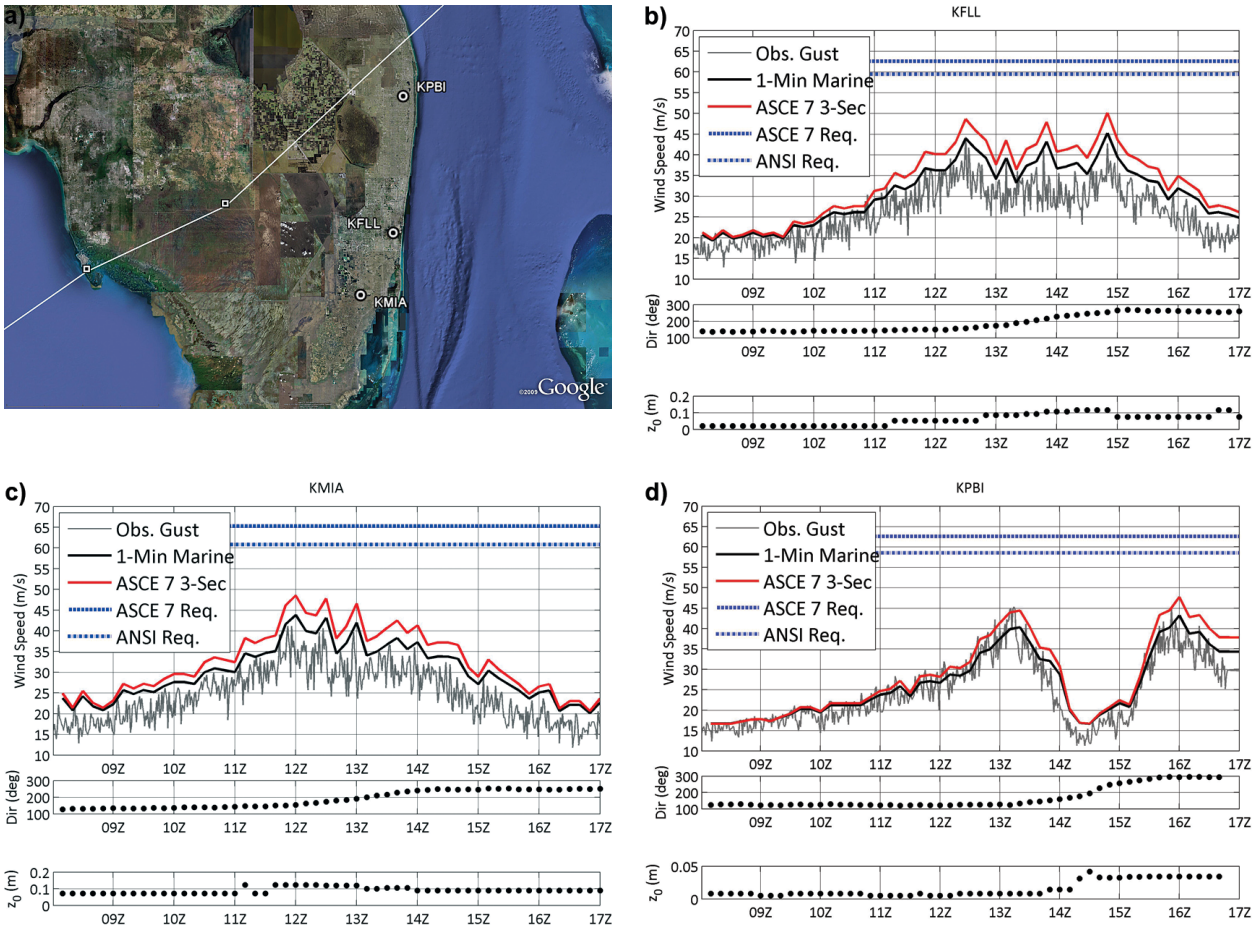

Fig. 12. (a) Hurricane Wilma's best track. (b)–(d) The conversion of observations measured at KFLL, KMIA, and KPBI during Hurricane Wilma (2005) to 1-min marine and open exposure conditions as defined by ASCE-7-10. Local design wind speed requirements for newer (ASCE-7) and older (ANSI) construction are depicted by blue lines. By either measure, it is evident that properties near these airports did not experience the nominal design wind speeds.

analysis tools, such as H*Wind, that already implement a standardization routine. For those that do not, it was shown that wind observations can be efficiently standardized to a common set of metadata. "Background" observational noise attributed to terrain effects and instrument response can be reduced to improve short-term forecast accuracy and real-time mesoscale analysis. Programs that can potentially benefit from this research are the Real-Time Mesoscale Analysis (www.nco.ncep.noaa.gov/pmb/nwprod/analysis) and the High-Resolution Rapid Refresh (http://ruc.noaa.gov/hrrr/), which were developed to serve users needing frequently updated, short-range forecasts at subkilometer scales. Standardization also has the potential to improve the initialization and verification of new and improved high-resolution operational hurricane forecast guidance models developed through NOAA's Hurricane Forecast Improvement Project.

The results demonstrate that the assumption that airports can be adequately described as open exposure will likely introduce errors into subsequent analyses. Only about one-third of the wind sectors were found to qualify as open exposure. The major implication is that users of the wind speed observations collected from the ASOSs should implement a postprocessing routine to standardize the data to a desired set of metadata (z, z_0, and t). The averaging duration and method vary by instrument on the ASOSs, and instrument heights vary from 8 to 11 m. The upwind fetch conditions range from marine to heavily built up and, with few exceptions, are heterogeneous in nature. Without a conversion, it has been shown that use of raw wind speed observations can introduce errors (underestimates) on the order of 40% relative to identical measurements made in standard conditions. Terrain effects and instrument response characteristics should be accounted for before surface

wind field observations can be compared or used to define intensity on a local scale.

It was shown that standardization enables meteorologists to convey the severity of an extreme wind event to the general public in terms of damage potential to a particular era of construction. The peak surface wind field intensity can be directly compared to nominal design values to determine if a "design level" event has occurred. Using the technique demonstrated herein, National Weather Service (NWS) Weather Forecast Offices can relay this information to interested parties (e.g., emergency response and recovery operations) during and after an event.

ACKNOWLEDGMENTS. The authors wish to acknowledge the University Scholars Program at the University of Florida for supporting Ms. Bacon in carrying out the research discussed herein. We also appreciate the helpful insights and suggestions provided by Dr. Anton Beljaars, European Centre for Medium-Range Weather Forecasts; Dr. Craig Miller, University of Western Ontario; and Dr. Mark Powell, NOAA's Hurricane Research Division.

REFERENCES

ASCE, 2010: Wind loads. *Minimum Design Loads for Buildings and Other Structures,* ASCE Standard Series, Vol. ASCE/SEI 7-10, ASCE, 241–258.

Ashcroft, J., 1994: The relationship between the gust ratio, terrain roughness, gust duration and the hourly mean wind speed. *J. Wind Eng. Ind. Aerodyn.,* **53,** 331–355.

Beljaars, A. C. M., 1987: The influence of sampling and filtering on measured wind gusts. *J. Atmos. Oceanic Technol.,* **4,** 613–626.

Bendat, J. S., and A. G. Piersol, 2000: Statistical principles. *Random Data: Analysis & Measurement Procedures,* Wiley-Interscience, 106–107.

Beven, J. L., II, and Coauthors, 2008: Atlantic hurricane season of 2005. *Mon. Wea. Rev.,* **136,** 1109–1173.

Bradley, E. F., 1968: Micrometeorological study of velocity profiles and surface drag in the region modified by a change in surface roughness. *Quart. J. Roy. Meteor. Soc.,* **94,** 361–379.

Busch, N. E., and L. Kristensen, 1976: Cup anemometer overspeeding. *J. Appl. Meteor.,* **15,** 1328–1332.

Choi, E. C. C., and F. A. Hidayat, 2002: Gust factors for thunderstorm and non-thunderstorm winds. *J. Wind Eng. Ind. Aerodyn.,* **90,** 1683–1696.

Davenport, A. G., 1964: Note on the distribution of the largest value of a random function with application to gust loading. *Inst. Civ. Eng. Proc.,* **28,** 187–196.

——, 1983: The relationship of reliability to wind loading. *J. Wind. Eng. Ind. Aerodyn.,* **13,** 3–27.

Deacon, E. L., 1953: Vertical profiles of the mean wind in the surface layers of the atmosphere. *Geophys. Mem.,* **91**.

Doggett, L., 1990: Sunrise/sunset algorithm. *Almanac for Computers,* Nautical Almanac Office, B5–B7. [Available online at http://williams.best.vwh.net/sunrise_sunset_algorithm.htm.]

Durst, C. S., 1960: Wind speeds over short periods of time. *Meteor. Mag.,* **89,** 181–186.

ESDU, 1983: Strong winds in the atmospheric boundary layer. Part 2: Discrete gust speeds, Engineering Sciences Data Unit 83045, 34 pp.

Greenway, M. E., 1979: An analytical approach to wind velocity gust factors. *J. Wind. Eng. Ind. Aerodyn.,* **5,** 61–91.

Grimmond, C. S. B., T. S. King, M. Roth, and T. R. Oke, 1998: Aerodynamic roughness of urban areas derived from wind observations. *Bound.-Layer Meteor.,* **89,** 1–24.

Harris, R. I., and D. M. Deaves, 1981: The structure of strong winds. *Proc. CIRIA Conf. on Wind Engineering in the Eighties,* London, United Kingdom, CIRIA, 4. [Available from CIRIA, Classic House, 174 - 180 Old Street, London EC1V 9BP, United Kingdom.]

Irwin, P. A., 2006: Exposure categories and transitions for design wind loads. *ASCE J. Struct. Eng.,* **132,** 1755–1763.

Kaimal, J. C., J. C. Wyngaard, Y. Izumi, and O. R. Coté, 1972: Spectral characteristics of surface-layer turbulence. *Quart. J. Roy. Meteor. Soc.,* **98,** 563–589.

Krayer, W. R., and R. D. Marshall, 1992: Gust factors applied to hurricane winds. *Bull. Amer. Meteor. Soc.,* **73,** 613–617.

Large, W. G., and S. Pond, 1981: Open ocean momentum flux measurements in moderate to strong winds. *J. Phys. Oceanogr.,* **11,** 324–336.

Lepage, M. F., and P. A. Irwin, 1985: A technique for combining historical wind data with wind tunnel tests to predict extreme wind loads. *Proc. Fifth U.S. National Conf. on Wind Engineering,* Lubbock, Texas, 2B-71–2B-78.

Lombardo, F. T., J. A. Main, and E. Simiu, 2009: Automated extraction and classification of thunderstorm and non-thunderstorm wind data for extreme-value analysis. *J. Wind. Eng. Ind. Aerodyn.,* **97,** 120–131.

Masters, F. J., H. W. Tieleman, and J. A. Balderrama, 2010: Surface wind measurements in three Gulf coast hurricanes of 2005. *J. Wind. Eng. Ind. Aerodyn.,* **98,** 533–547.

Mehta, K. C., 1984: Wind load provisions of ANSI #A58.1-1982. ASCE J. Struct. Eng., **110,** 769–784.

Miller, C. A., 2007: Defining the effective duration of a gust. *Proc. 12th Int. Conf. on Wind Engineering,* Cairns, QLD, Australia, IAWE, 759–766.

NWS, 2003: ASOS product improvement implementation plan for ice free wind, addendum III. NWS Rep., 76 pp. [Available online at www.weather.gov/ops2/Surface/documents/IFW030515A.pdf.]

Orwig, K. D., and J. L. Schroeder, 2007: Near-surface wind characteristics of extreme thunderstorms. *J. Wind. Eng. Ind. Aerodyn.,* **95,** 565–584.

Pasquill, F., 1961: The estimation of the dispersion of windborne material. *Meteor. Mag.,* **90,** 33–49.

Powell, M. D., S. Houston, and T. A. Reinhold, 1996: Hurricane Andrew's landfall in South Florida. Part I: Standardizing measurements for documentation of surface wind fields. *Wea. Forecasting,* **11,** 304–328.

——, ——, L. R. Amat, and N. Morisseau-Leroy, 1998: The HRD real-time hurricane wind analysis system. *J. Wind Eng. Ind. Aerodyn.,* **77 & 78,** 53–64.

——, P. J. Vickery, and T. A. Reinhold, 2003: Reduced drag coefficients for high wind speeds in tropical cyclones. *Nature,* **422,** 279–283.

——, D. Bowman, D. Gilhousen, S. Murillo, N. Carrasco, and R. St. Fleur, 2004: Tropical cyclone winds at landfall: The ASOS–C-MAN wind exposure documentation project. *Bull. Amer. Meteor. Soc.,* **85,** 845–851.

Saffir, H., 1975: Low-cost construction resistant to earthquakes and hurricanes. Department of Economic and Social Affairs Rep. ST/ESA/23, United Nations, 205 pp.

Schmitt, C. V., IV, 2009: A quality control algorithm for the ASOS ice free wind sensor. Preprints, *13th Conf. on Integrated Observing and Assimilation Systems for Atmosphere, Oceans, and Land Surface,* Phoenix, AZ, Amer. Meteor. Soc., 12A.3. [Available online at http://ams.confex.com/ams/89annual/techprogram/paper_145755.htm.]

Sheppard, P. A., 1947: The aerodynamic drag of the earth's surface and the value of von Karman's constant in the atmosphere. *Proc. Roy. Soc. London,* **A188,** 208–222.

Simiu, E., P. Vickery, and A. Kareem, 2007: Relation between Saffir-Simpson hurricane scale wind speeds and peak 3-s gust speeds over open terrain. *J. Struct. Eng.,* **133,** 1043–1045.

Simpson, R. H., 1974: The hurricane disaster potential scale. *Weatherwise,* **27,** 169–186.

Tieleman, H., 1995: Universality of velocity spectra. *J. Wind. Eng. Ind. Aerodyn.,* **56,** 55–69.

Uhlhorn, E. W., P. G. Black, J. L. Franklin, M. Goodberlet, J. Carswell, and A. S. Goldstein, 2007: Hurricane surface wind measurements from an operational stepped frequency microwave radiometer. *Mon. Wea. Rev.,* **135,** 3070–3085.

Van der Hoven, I., 1957: Power spectrum of horizontal wind speed in the frequency range from 0.0007 to 900 cycles per hour. *J. Meteor.,* **14,** 160–164.

Vickery, P. J., and P. F. Skerlj, 2005: Gust factors revisited. *J. Struct. Eng.,* **131,** 825–832.

Wieringa, J., 1973: Gust factors over open water and built-up country. *Bound.-Layer Meteor.,* **3,** 424–441.

Yamartino, R. J., 1984: A comparison of several "single pass" estimators of the standard deviation of wind direction. *J. Climate Appl. Meteor.,* **23,** 1362–1366.